JOURNAL OF AGRICULTURAL AND FOOD CHEMISTRY

Article

pubs.acs.org/JAFC

Decomposition Pathways and Rates of Human Urine in Soils

Federico Maggi*,† and Edoardo Daly‡

†School of Civil Engineering, Building J05, The University of Sydney, Sydney, NSW 2006, Australia

‡Department of Civil Engineering, Monash University, Clayton, VIC 3800, Australia

ABSTRACT: This study proposes a comprehensive reaction network of the soil microbial breakdown of the main compounds in human urine to the end products NH_3 and NH_4^+. A reactive model was developed and parameters were determined against experimental data. The model was used to assess the amount and release rate of NH_3 and NH_4^+ in a soil control volume flushed with (i) pulses of urine at various dilutions and (ii) a continuous flow of urine at various dilutions and flow rates. In scenario i, 90% of incoming organic nitrogen was converted to NH_3 and NH_4^+ between 5 and 20 days from application at rates strongly dependent on the initial microbial soil content. Urea and hippuric acid were largely correlated to NH_3 and NH_4^+ release, whereas microbial functional groups in the same scenarios were poorly correlated with NH_3 and NH_4^+ release. In scenario ii, 90% conversion was generally reached for low flow rates and was highly nonlinear with the dilution. Finally, a stochastic analysis showed that urine decomposition was more sensitive to uncertainty in microbial growth rate parameters than half-saturation concentrations.

KEYWORDS: *decomposition, urine, soil, urbanization*

INTRODUCTION

The rapid population growth and urbanization rates are calling for more sustainable uses of resources and management of wastes. These may include the recycling of human excreta, which are rich in nutrients and available in large amounts in metropolitan areas.[1−3] Human excreta have been used as organic fertilizer since ancient times,[4] and their use in agriculture is still common practice in areas around the world, such as many parts of Southeast Asia,[5] Africa,[6] and several other developed and developing countries. Estimates in refs 7 and 8 suggested that the annual per capita amount of human excreta would correspond to the fertilizer required for the production of about 250 kg of cereal.

The reuse of human urine is specifically receiving increasing attention as an alternative fertilizer because it contains most of the nutrients of human excreta[9] and it can yield considerable amounts of nitrogen (N), phosphorus (P), potassium (K), sulfur (S), calcium (Ca), and magnesium (Mg). According to refs 9 and 10 urine could substitute up to 37% of N, 20% of P, and 15% of K from mineral fertilizers. Major concerns limiting urine reuse are related to health risks associated with pathogenic cross-contamination from feces and societal acceptance, especially in developed countries. Regardless of health risk issues (not treated here), knowledge of the performance of human urine to flank, if not replace, mineral fertilization in agriculture is still limited. Some studies showed successful use of urine for crop fertilization. Kirchmann and Pettersson[11] were among the first to show, in pot experiments with barley, that the fertilizing efficiency of human urine for P was higher than that of amendments of solute P, whereas it was somehow lower for N due to losses by volatile N forms. In field experiments, it was shown that urine applications resulted in similar plant growth characteristics as compared to those using mineral fertilizers[12] or led to enhanced plant height and leaf length in maize.[13] Likewise, tests on tomatoes,[14,15] red beet,[16] pumpkin,[17] maize,[6,18] and okra crops[19] showed very similar results, all reporting an increased plant biomass as compared to no fertilization and a yield comparable to or higher than that from mineral fertilizers. Pradhanetal et al.[12] also reported that the biological attack on plants was substantially lower in urine-fertilized cabbage than in the control cabbage (with no or mineral fertilization).

These studies support with growing evidence that the use of human urine in agriculture may be feasible. However, in addition to experimental studies, improved knowledge of the catabolic breakdown of urine compounds when applied to soils is required to help in the development of mathematical models able to quantify and predict the amounts of urine necessary to meet plant uptake and to achieve planned crop yields.

This work starts filling in these knowledge gaps by (i) proposing a reaction network of the decomposition pathways in soils of the main compounds detected in human urine, with a particular emphasis on those leading to N end-products, (ii) estimating the reaction parameters using experimental data, and (iii) developing a model to quantify the release rate of N end-products that will be available for plant uptake.

Although simplified, the proposed reaction network accounts for dissolved compounds that collect up to 90% of the mass in human urine and represents the most complete reaction structure of human urine breakdown in soils to the best of our knowledge. The model developed on the basis of this reaction network includes mechanisms sufficient to capture the main urine cycle dynamics and fills in the current lack of mechanistic accounting of the dominant processes that determine the release rate and timing of NH_3 and NH_4^+ following urine application to soils. The model was used to analyze (i) the transient state of each urine component over time after an

Received: March 18, 2013
Revised: June 7, 2013
Accepted: June 10, 2013
Published: June 10, 2013

instantaneous application of urine and (ii) the steady state associated with continuous urine amendment at various flow rates and dilutions. A stochastic sensitivity analysis focused on parameter uncertainty.

MATERIALS AND METHODS

Major Compounds of Human Urine. To date, the most comprehensive list of compounds and analysis of physicochemical characteristics of human urine is found in the NASA report compiled by Putnam.[20] Human urine is a mixture of more than 200 compounds, which include electrolytes, nitrogenous, phosphorus, and sulfur compounds, vitamins, hormones, organic acids, and other organic and inorganic compounds.[20] Of the 158 measured compounds, about 70 have concentration >10 mg/L and correspond to a mass of about 36.8 g/L; the remaining components represent approximately 0.25 g/L. The elemental composition of the total dissolved solids in human urine includes 6.87 g/L carbon (C), 8.12 g/L nitrogen (N), 8.25 g/L oxygen (O), 1.51 g/L hydrogen (H), and 0.13 g/L organic sulfur (S) (Table 3 in Putnam[20]).

The most abundant compounds among those reported in Putnam[20] are listed in Table 1 in order of decreasing concentration under the three classes of organic amino compounds (OACs), organic ammonium salts (OASs), and inorganic salts (ISs). In Table 1, OACs were selected from the effective ensemble of compounds detected in human urine, OASs were referenced in ref 20 as equivalent to a proposed concentration of solute ammonia $NH_3(aq)$, and ISs were referenced to be equivalent to a proposed concentration of K^+, Na^+, Cl^-, SO_4^{-2}, and HCO_3^- ions.

Table 1. Summary of Major Organic Amino Compounds (OAC), Organic Ammonium Salts (OAS), and Inorganic Salts (IS) Present in Human Urine[20] (Sorted by Decreasing Concentrations)

		atomic composition	mol wt (g/mol)	concn (mg/L)
OAC				
	urea	CH_4ON_2	60.1	9300−23300
	creatinine	$C_4H_7ON_3$	113.1	670−2150
	hippuric acid	$C_9H_9O_3N$	179.0	50−1670
	uric acid	$C_5H_4O_3N_4$	168.1	40−670
	tyrosine	$C_9H_{11}O_3N$	181.2	70−560
	creatine	$C_4H_9O_2N_3$	149.2	0−530
	glycine	CH_9O_2N	75.1	90−450
OAS				
	hippurate	$C_9H_{12}O_3N_2$	196.2	1250
	citrate	$C_6H_{14}O_7N_2$	226.2	756
	glucuronate	$C_6H_{13}O_7N$	211.1	663
	urate	$C_5H_7O_3N_5$	185.1	518
	lactate	$C_3H_{13}O_3N_2$	127.1	394
	equivalent to	NH_3	17	200−730
IS				
	sodium chloride	NaCl	58.4	8001
	potassium sulfate	K_2SO_4	174.3	2632
	potassium chloride	KCl	74.6	1641
	potassium bicarbonate	$KHCO_3$	100.1	661
	equivalent to	Cl^-	35.5	1870−8400
		Na^+	23.0	1170−4390
		K^+	39.1	750−2610
		SO_4^{2-}	64.1	154−940
		HCO_3^-	61.0	20−560

Reaction Network. The OACs, OASs, and ISs listed in Table 1 were included in the reaction network of Figure 1, where their chemical and biological breakdown were represented along pathways resulting in ionic end products. In this reaction network, we propose two major pathways: one involves biochemical reactions driven by microbially synthesized enzymes for OACs, and the other involves only chemical reactions for OASs and ISs.

Biochemical pathways correspond to catabolic reactions that break OACs with higher stoichiometric C content down to compounds with sequentially lower C content. Starting from tyrosine (uropepsin) and hippuric acid, that is, the two compounds with the greatest stoichiometric C content, the reaction network reached the simplest carbohydrate monomer CH_2O (Table 1). During each breakdown step, intermediate amino compounds are formed until the ultimate release of NH_3 and NH_4^+.

Tyrosine is formed in the human stomach, and a small fraction of it is excreted by kidneys.[21] Tyrosine biological breakdown by soil microorganisms has not been thoroughly investigated yet; hence, the exact intermediate and final products are not clearly known, and breakdown rates are not available. It is likely that NH_3 appears as a final product and that several intermediate compounds are formed, although they are not yet detected and identified within the context of soil biogeochemistry. We assume that urea (CH_4ON_2) is one of the representative intermediate compounds (see assumed pathway depicted by dashed line in Figure 1). According to this assumption, the breakdown of tyrosine to urea by soil microorganisms can be expressed by means of the oxidation reaction

$$\underset{\text{tyrosine}}{C_9H_{11}O_3N} + \frac{19}{2}O_2 \rightarrow \frac{1}{2}\underset{\text{urea}}{CH_4ON_2} + \frac{9}{2}H_2O + \frac{17}{2}CO_2 \quad (1)$$

Other pathways, such as direct breakdown to NH_3 (see hypothesized pathway depicted by dotted line in Figure 1) are possible, but they were not investigated further.

Similarly to tyrosine, the biological decomposition of hippuric acid has not been investigated in depth yet. As such, we assumed that hippuric acid is decomposed first to urea and then to NH_3. Oxidation of hippuric acid can thus be written as

$$\underset{\text{hippuric acid}}{C_9H_9O_3N} + 9O_2 \rightarrow \frac{1}{2}\underset{\text{urea}}{CH_4ON_2} + \frac{7}{2}H_2O + \frac{17}{2}CO_2 \quad (2)$$

Figure 1 also depicts direct biological decomposition of hippuric acid to NH_4^+, but the corresponding reaction was not explicitly included in the work presented here.

Uric acid was shown to entirely decompose to NH_3 under the action of enzymes produced by some *Pseudomonas* groups in aerobic soils.[22] A pathway that involves several intermediate OACs, including urea, to the ultimate formation of NH_3 is likely. Although those intermediates may have a role in determining the time scale of NH_3 release, only urea was explicitly taken into account here as the most important among them. Uric acid decomposition in soils occurs mostly as an aerobic reaction performed by various bacterial strains,[23] whereas anaerobic decomposition is known to be mediated only by one strain.[24] In aerobic conditions, most strains were found to convert uric acid to urea, and only a minority of bacterial strains decomposed uric acid to NH_3. Excluding anaerobic decomposition and direct decomposition to NH_3, the reaction of uric acid decomposition to urea proposed here follows from Bachrach[22] and is

$$\underset{\text{uric acid}}{C_5H_4O_3N_4} + 2H_2O + \frac{3}{2}O_2 \rightarrow 2\underset{\text{urea}}{CH_4ON_2} + 3CO_2 \quad (3)$$

Figure 1 also includes direct decomposition to ammonium ion, but the reaction was not explicitly used in the work presented here.

Creatine and creatinine are known to undergo a reversible enzymatic hydrolysis reaction as[25−27]

$$\underset{\text{creatine}}{C_4H_9O_2N_3} \rightleftharpoons \underset{\text{creatinine}}{C_4H_7ON_3} + H_2O \quad (4)$$

Although both compounds can be decomposed by anaerobic bacteria in soils (mainly *Pseudomonas*), studies focused mainly on crea-

dx.doi.org/10.1021/jf401212n | J. Agric. Food Chem. 2013, 61, 6175−6186

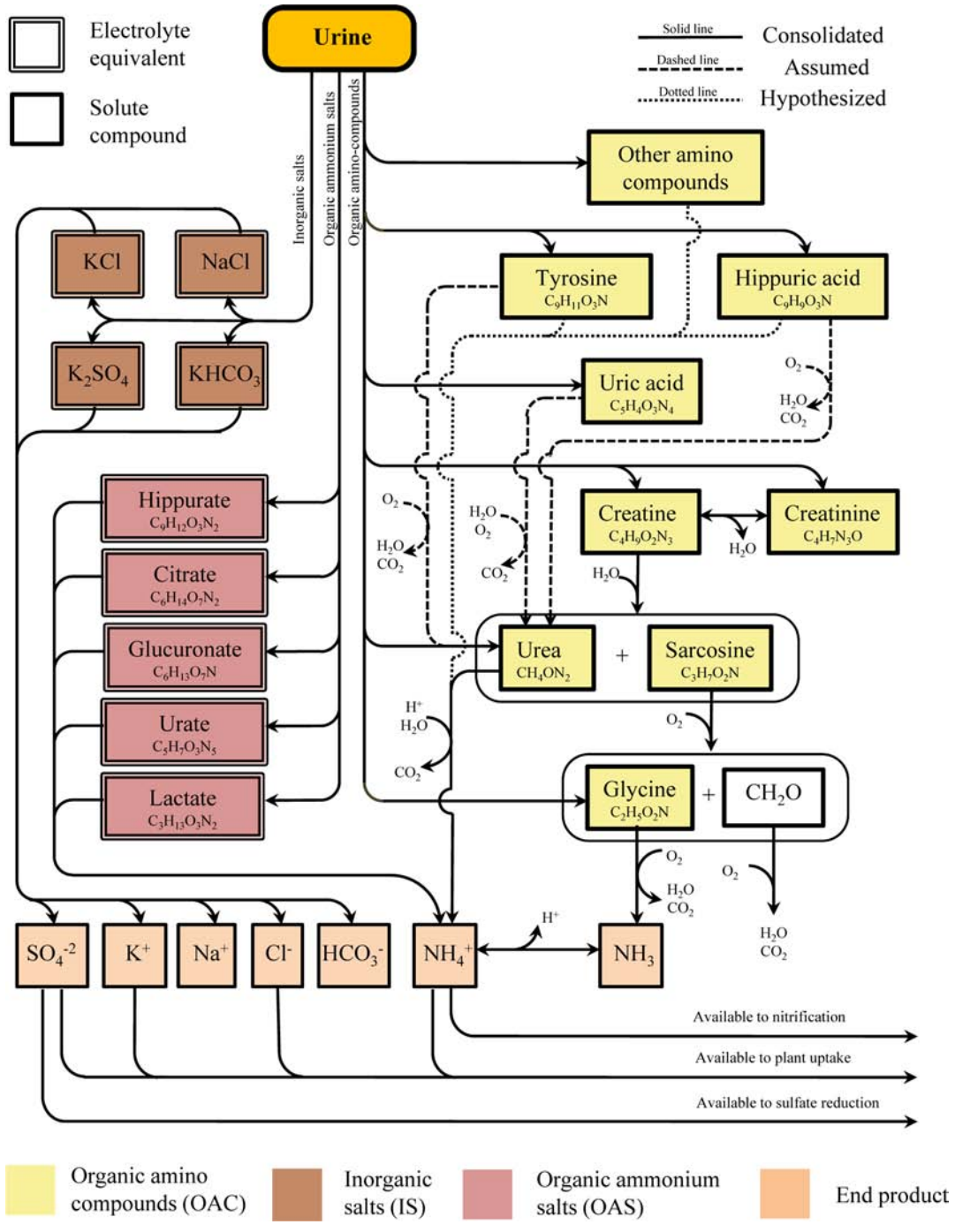

Figure 1. Representation of chemical and biochemical breakdown pathways of major compounds found in human urine.

tine,[26,28,29] and a large consensus was found on the identification of urea and sarcosine ($C_3H_7O_2N$) as end-products.[30,31] Biologically mediated decomposition of creatine can be written as a hydrolysis reaction as[26]

$$\underset{\text{creatine}}{C_4H_9O_2N_3} + H_2O \rightarrow \underset{\text{urea}}{CH_4ON_2} + \underset{\text{sarcosine}}{C_3H_7O_2N} \quad (5)$$

Sarcosine is normally absent in human urine from healthy individuals, but it results from the decomposition of creatine. Sarcosine was observed to be consumed to glycine ($C_2H_5O_2N$) concurrently with O_2 uptake by *Pseudomonas ovalis* strain.[30] Sarcosine oxidation to glycine can be written as

$$\underset{\text{sarcosine}}{C_3H_7O_2N} + \frac{1}{2}O_2 \rightarrow \underset{\text{glycine}}{C_2H_5O_2N} + CH_2O \quad (6)$$

where CH_2O is a carbohydrate monomer next oxidized to CO_2[30] (Figure 1).

Glycine produced from sarcosine breakdown was shown to be oxidized by *P. ovalis* similarly to sarcosine in aerobic conditions, leading to NH_3 as a final product.[30] The reaction of glycine oxidation can be written as

$$\underset{\text{glycine}}{C_2H_5O_2N} + \frac{3}{2}O_2 \rightarrow NH_3 + H_2O + 2CO_2 \quad (7)$$

Urea is the urine compound with the highest concentration. Although present as free compound, urea results also from the decomposition of creatine and, according to our reaction chain, from tyrosine, hippuric acid, and uric acid. Chemical breakdown of urea has been investigated for more than a century,[32] and hydrolysis is the most

dx.doi.org/10.1021/jf401212n | J. Agric. Food Chem. 2013, 61, 6175−6186

widely accepted reaction responsible for its degradation.[33] It is now known that urea undergoes both chemical and biochemical hydrolysis reactions, the former being substantially slower than the latter.[34] In soils, several bacterial strains can lead to complete urea hydrolysis to NH_3 via the amidohydrolase enzyme[35] by the reaction

$$\underset{\text{urea}}{CH_4ON_2} + 2H^+ + H_2O \rightarrow 2NH_4^+ + CO_2 \tag{8}$$

Finally, the end-products of glycine and urea decomposition were described to be in equilibrium according to the chemical reaction

$$NH_4^+ \rightleftharpoons NH_3 + H^+ \tag{9}$$

The reaction network in Figure 1 included aqueous OASs and ISs, which were assumed to directly dissociate to NH_4^+, SO_4^{-2}, K^+, Cl^-, Na^+, and HCO_3^- ions. Of these ions, the first three are nutrients taken up by plants,[36] whereas the last three are normally toxicant to plants at variably high concentrations.[37] Additionally, it is noted that NH_4^+ feeds nitrification reactions[38,39] and SO_4^{-2} feeds sulfate reduction reactions.[40] We recall here that biogeochemical reactions of these ions and plant uptake were beyond the aim of this study and were not included in the analytical part.

Equilibrium and Kinetic Equations. Dissociations between creatine and creatinine as well as NH_3 and NH_4^+ were assumed to occur rapidly enough to be considered equilibrium reactions; hence, they were fully determined by an equilibrium constant.[41]

Biological decomposition of tyrosine, hippuric acid, uric acid, creatine, sarcosine, glycine, and urea was described with Michaelis–Menten kinetics coupled with Monod microbial biomass dynamics.[42,43] Consider a generic reaction $x\mathrm{X} \overset{B_X}{\rightarrow} p\mathrm{P}$, controlled by the biomass B_X, with the generic substrate X and product P, stoichiometric coefficients x and p, and under the assumption that other reactants (e.g., O_2) are not limiting the reaction. The rate of change of substrate and product concentrations, $C_X(t)$ and $C_P(t)$, and the biomass concentration, $B_X(t)$, at time t were modeled using modified Michaelis–Menten–Monod ordinary differential equations as

$$\frac{dC_X(t)}{dt} = -x\mu_X \frac{C_X(t)}{C_X(t) + K_X}\frac{B_X(t)}{Y_X} + S_X \tag{10a}$$

$$\frac{dC_P(t)}{dt} = p\mu_X \frac{C_X(t)}{C_X(t) + K_X}\frac{B_X(t)}{Y_X} + S_P \tag{10b}$$

$$\frac{dB_X(t)}{dt} = x\mu_X \frac{C_X(t)}{C_X(t) + K_X} I(t)B_X(t) - \delta_X B_X(t) \tag{10c}$$

where μ is the reaction rate constant, K is the Michaelis–Menten half-saturation concentration, Y is the biomass yield coefficient describing the biomass gain per mole of consumed substrate, δ is the biomass mortality rate, and the subscript $_X$ expresses the above parameters relative to compound X. The terms S_X and S_P are sources of component X and P. The inhibition term I in eq 10c was introduced to limit biomass growth to the soil biomass carrying capacity. In fact, in ideally pure cultures under unlimited nutrient availability and in the absence of biological competitors (e.g., grazers) or chemical inhibitors, biomass can grow indefinitely until all space is occupied. In soils, growth is limited by pore space. Experiments in artificial porous media showed an initial exponential biomass growth, which underwent a logistic-type progression until growth ceased when pores were clogged.[44,45] On the basis of those observations and the mathematical model in Maggi and Porporato,[46] the soil carrying capacity relative to space was set to be proportional to the pore volume; accordingly, the logistic-type inhibition factor in eq 10c was expressed as

$$I(t) = 1 - f_b \frac{\sum B_X(t)}{s_B \phi V} \tag{11}$$

where the sum is extended to all microbial functional groups, ϕ is the soil porosity, s_B is the biomass saturation representing the fraction of soil pores available to cells, and V is the soil control volume. The coefficient $f_b = 0.8 \times 10^{-6}$ L mg^{-1} (liters of water per milligrams of cell) was used to convert the microbial biomass concentration to volume of biomass water assuming that about 80% of microorganismal cell mass was made of water.[47] The volume V as well as the porosity ϕ and biomass saturation s_B are detailed in the next sections.

The equilibrium and kinetic equations describing the reaction network in Figure 1 were integrated in a system of ordinary differential equations to describe the urine cycle in soils (see the Appendix for the expanded set of equations relative to each compound). In both the direct and inverse problem solution of the equations, an implicit finite difference method with variable integration time step was used. Mass conservation was verified in all simulations.

Experimental Data and Parameter Estimation. The ratio of creatinine to creatine concentration in eq 4 was experimentally found to be in equilibrium at 42.5/57.5 parts;[27] thus, the equilibrium constant $pk_d = -0.302$ mol L^{-1}. The equilibrium constant $pk_d = -9.241$ mol L^{-1} between NH_4^+ and NH_3 in eq 9 was taken from the EQ3/6 thermodynamic database.[48]

Several existing experimental data were used to determine the values of μ_X, K_X, Y_X, and δ_X for the biodecomposition kinetic reactions. Specifically, tyrosine and hippuric acid decomposition in eqs 1 and 2 were determined upon experimental data in ref 49, which measured the changing concentration of hippuric acid from the time of application to a soil sample over about a 1 month period. Experimental data relative to tyrosine decomposition in soils were not found in the existing literature; hence, the values of μ and K relative to hippuric acid were used as a first approximation for those of tyrosine. The assumption was taken on the basis that the C atom numbers in hippuric acid and tyrosine are identical and that oxidation of these compounds could be occurring at similar rates.

The kinetic reaction of uric acid biodecomposition in eq 3 was determined upon experimental incubation of soil bacteria (uncharacterized *Pseudomonas*) growing on uric acid as the only source of C, N, and energy.[22]

Creatine decomposition to urea and sarcosine in eq 5, sarcosine decomposition to glycine in eq 6, and glycine decomposition to NH_3 in eq 7 were determined against experiments conducted using enzymes extracted from a suspension of *P. ovalis* cells in a solution of creatine, sarcosine, and glycine. O_2 uptake was measured by chromatography at various times during oxidation of these substrates.[30]

Finally, urea decomposition to NH_3 in eq 8 was determined using data in ref 50 which measured the urea concentration after an initial amendment in a saturated loam over a period of about 5 days.

The values of experimental concentrations were used to determine the kinetic parameters in eqs 10, and the initial microbial biomass concentration $B_X(t = 0)$ specifically growing on compound X; the initial concentrations, $C_X(t = 0)$, were known from the same experiments described before. For parameter estimation, the trust-region-reflective minimization algorithm provided in the MATLAB2011b package (i.e., function "lsqcurvefit") was used against experimental data introduced above. The parameters were constrained within arbitrary bounds; for example, the biomass yield coefficient was limited to a maximum of 1 g C-bio g C-sub^{-1} (grams C biomass per gram C substrate) after measurements in ref 51 and was independently estimated in individual reactions. Earlier observations of the survival time of various soil bacteria ranged between 24 h and 2–3 weeks, which corresponded to mortality rates between about 10^{-5} and 5×10^{-7} s^{-1}.[52] An average biomass mortality rate was set to 10^{-6} s^{-1} for all microbial functional groups in the reaction network of Figure 1 after refs 53 and 54. An average mortality rate was used assuming that cell aging occurred with the same rate because the various microorganisms belonged to similar taxonomic groups and because the balance between biomass gain and loss was rather determined by substrate-dependent biomass growth rate. We note, though, that the actual aging variability may depend on strain-, chemical-, and environment-specific factors as well as on symbiotic and competitive features between various microbial soil communities, which were not explored in this work.

Finally, minimization during parameter estimation was considered to be successful when the global minimum was found.

Table 2. Summary of Parameters Relative to Biological Decomposition Reactions of Tyrosine (Tyr), Hippuric Acid (HA), Uric Acid (UA), Creatine (Cr), Sarcosine (Src), Glycine (Gly), and Urea, Respectively

reaction	x	p	C atoms	μ (s^{-1}) × 10^{-6}	K (mol/L)	Y [(g C-bio)/(g C-sub)]	Y [(mg bio)/(mg sub)]	δ (s^{-1}) × 10^{-6}
Tyr → urea	1	0.5	9	1.51	1.28	2.72×10^{-4}	2.93×10^{2}	1.00
HA → urea	1	0.5	9	1.51	1.28	2.72×10^{-4}	2.93×10^{2}	1.00
UA → urea	1	2	5	8.72	3.31×10^{-1}	9.39×10^{-4}	5.63×10^{2}	1.00
Cr → Src + urea	1	1	4	2.84	4.58×10^{-4}	4.82×10^{-2}	2.32×10^{4}	1.00
Src → Gly	1	1	3	4.04	1.90×10^{-3}	4.26×10^{-1}	1.53×10^{5}	1.00
Gly → NH_3	1	1	2	2.85	7.29×10^{-3}	3.73×10^{-1}	8.95×10^{4}	1.00
urea → NH_4^+	1	2	1	8.88	1.52×10^{-3}	2.77×10^{-1}	3.33×10^{4}	1.00

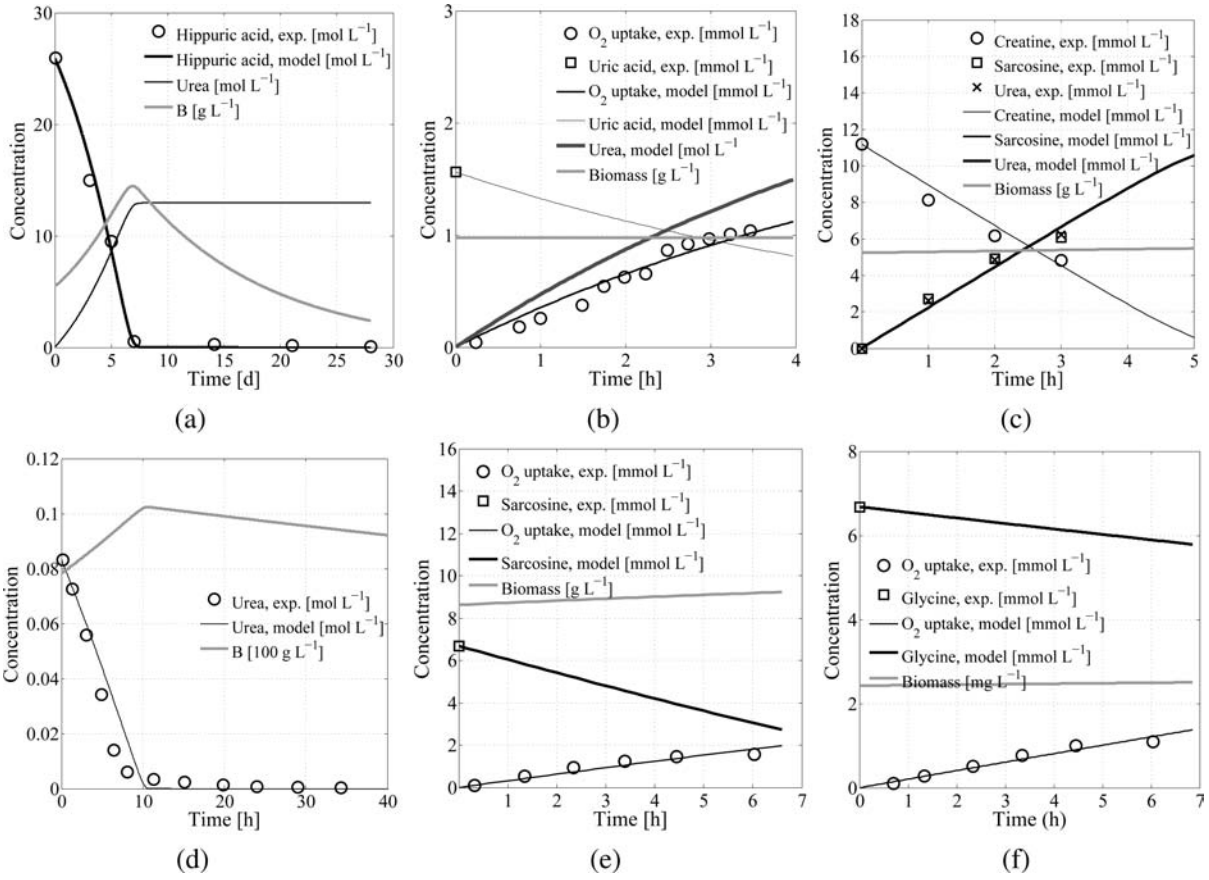

Figure 2. Experimental and modeled biological decomposition of (a) hippuric acid, (b) uric acid, (c) creatine, (d) urea, (e) sarcosine, and (f) glycine. Experimental data are (a) from ref 49, (b) from ref 22, (c, e, and f) from ref 30, and (d) from ref 50.

Modeling Urine Cycle in Soils. The equilibrium and kinetic equations describing the reaction network in Figure 1 were used with a bucket model consisting of a soil control volume with the aqueous OAC concentration of Table 1 calculated as a function of the urine inflow rate and degradation reactions estimated above. The soil minerals and moisture content were assumed to be homogeneous in the control volume. It was also assumed that the soil water volume was constant and totaled V_w = 1 L and that it was at field capacity (ψ = −0.33 bar = −336.5 cm); that is, any liquid amendment would result in leaching. For an average clay loam made of 30% sand, 35% silt, and 35% clay, with a porosity ϕ = 45.1%, air-entry suction ψ_s = −30.7 cm, and pore volume distribution index b = 8.4,[55] a water content of about θ = 0.34 m^3 m^{-3} was estimated using the water retention curve in ref 56, corresponding to the saturation $S = \theta/\phi$ = 0.75. The soil control volume was therefore $V = V_w/\theta$ = 2.9 L. The inflow rate of urine compounds was arbitrarily controlled by the volumetric urine flow rate, F, which in turn determined the soil moisture turnover time as $T = V_w/F$. A urine dilution factor, D, was used to control the absolute inflow mass rate of OACs. For example, the mass flow rate F_X of component X was determined as

$$F_X = DC_X^* F \tag{12}$$

with C_X^* the natural average concentration of component X in human urine from Table 1. The effluent mass E_X of each OAC was calculated over time as

$$E_X(t) = C_X(t)F \tag{13}$$

where $C_X(t)$ was determined by the biochemical reactions described in eqs 10. We assumed that microorganisms were not exchanged to and from the control volume because human urine does not normally contain microorganisms in healthy individuals and because these normally live attached to the mineral phase. The source term S_X (and S_P analogously) was written as a function of F as

$$S_X = \frac{F_X}{V_w} = DC_X^* \frac{F}{V_w} \tag{14}$$

Finally, a biomass saturation s_B = 0.4 was assumed, meaning that cells could grow up to 40% of the pore volume. In fact, complete clogging in soils is not likely because of environmental factors such as a

dx.doi.org/10.1021/jf401212n | J. Agric. Food Chem. 2013, 61, 6175−6186

very wide pore size spectrum, redox conditions, chemical and biochemical repellents, microbial grazing, and nutrient limitation and competition.

Gaseous and aqueous O_2 were not included in the model as these were assumed not to be limiting in the soil top 50 cm, where the $O_2(g)$ partial pressure decreases only marginally as compared to the atmosphere and where urine is assumed to be applied. Similarly, additional processes of uptake of end-products of Figure 1 were not included as this work mainly focused on demonstrating the productivity rate of nutrients required by soil microorganisms and plants.

RESULTS

Estimated Biochemical Parameters. The parameters determining the kinetic reactions relative to OACs are summarized in Table 2.

In qualitative terms, estimated parameters and the accuracy of the model in reproducing the measured concentrations in Figure 2 were deemed acceptable in relation to the scope of our work.

The estimated rate constants ranged within a relatively narrow band of values from about 1.51×10^{-6} s^{-1} to about 8.88×10^{-6} s^{-1} (Table 2). Conversely, the Michaelis−Menten half-saturation concentrations K_X spanned a large range of values from about 4.58×10^{-4} to 1.28 mol L^{-1}. Typically, K_X in chemical reactions represents the substrate concentration that results in half-reaction velocity as compared to its maximum, μ_X. However, the reaction velocity in biochemical reactions is also proportional to the biomass content, which varies over time as per eq 10c. Hence, there is no straightforward approach that can anticipate a value for K_X. The parameters in Table 2 show that no clear correlation existed between K_X, the maximum specific reaction rate μ_X, and the biomass yield Y_X. However, one may rather infer from Table 2 that K_X generally decreased with a decreasing C content in the various OAC substrates. Likewise, the estimated biomass yield Y_X, when expressed by C fraction, was low for C-rich compounds and high for C-depleted compounds. This agreed with the paradigm that microorganisms assimilate and preferably grow on simpler (lower C) rather than more complex (higher C) compounds.

Pulse Amendments. Simulations were carried out to investigate the degradation time scale of OAC compounds and the related dynamics of microbial decomposers over a period of 30 days following an application of 1 L of urine as an instantaneous (pulse) application. The overall urine dynamics for pulse amendments are necessarily strongly dependent on the initial and incoming OAC concentration, as well as the initial microbial biomass concentration. On the one hand, a high OAC initial concentration could result in higher biological activity, whereas decomposers could require a longer time to convert OACs to NH_3 and NH_4^+ when the OAC concentration decreases. On the other hand, amendments of diluted urine could lead to slower or faster reaction rates depending on the initial microbial content.

To explore the effect of OAC concentrations on urine degradation, a set of simulations was run with the dilution factor D ranging from 0.1 to 1 (diluted OACs) and from 1 to 10 (concentrated OACs). The biomass concentration for each microbial functional group was initialized at $B_X(t = 0) = 100$ mg L^{-1}. A net conversion factor f_{con} was calculated as

$$f_{con}(t) = \frac{[NH_3(t)] + [NH_4^+(t)]}{\sum_X m_X[C_X(t)]} - \frac{[NH_3(0)] + [NH_4^+(0)]}{\sum_X m_X[C_X(0)]} \quad (15)$$

where m_X is the molar N content in compound X and the sum is extended to all OACs; f_{con} expresses the ratio between the N moles in the end-products NH_3 and NH_4^+ and the N moles in the control volume over time relative to the initial N ratio.

The colored map of Figure 3 shows that a net 50% of the total N was converted to assimilable NH_3-N and NH_4^+-N in about 2−3 days ($D \simeq 0.1$) and not later than about 8 days ($D \simeq 10$) after amendment. At high urine concentrations ($D \simeq 10$), 90% conversion was reached no later than about 20 days. After 20 days, further conversion to NH_3 and NH_4^+ was very slow or negligible because of a low OAC residual concentration. Overall, the biogeochemical degradation of a pulse of human urine extended for no more than 20−30 days after application, when at least 90% of the total N introduced by an amendment of urine was converted to NH_3 and NH_4^+.

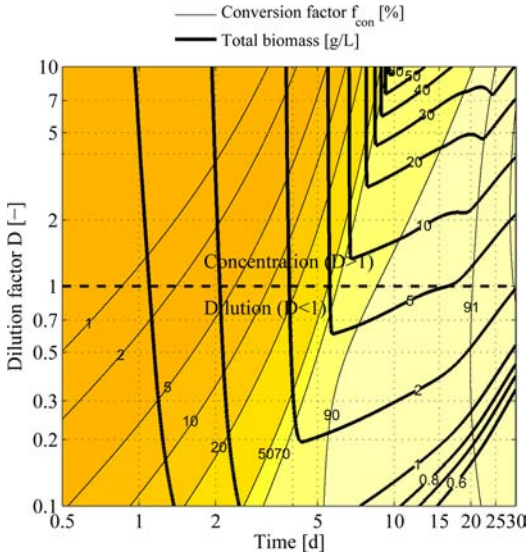

Figure 3. Modeled net conversion factor f_{con} of total N to NH_3−N and NH_4^+-N (colored area) and total microbial biomass (thick black lines) over 30 days following an instantaneous application of 1 L of human urine in soils for dilutions D between 0.1 and 10 and an initial concentration of 100 mg L^{-1} of each microbial functional group.

The total biomass (thick black lines in Figure 3) increased from <1 g L^{-1} to about 60 g L^{-1} at $D = 10$ after about 8 days from urine application. Figure 3 also shows that the maximum biomass content emerged for any given dilution D when the conversion factor f_{con} was between 80 and 90%; after that maximum, the total biomass concentration decreased. An increasing D generally enhanced the total biomass production.

With the capability to track all chemical and biological components, the concentrations of each individual OAC and microbial group are represented in Figure 4a,b for $D = 1$. These panels show that tyrosine and hippuric acid were consumed slowly as per experiments in Figure 2a, thus suggesting that complex organic compounds were assimilated by microorganisms at a slow rate. Tyrosine, hippuric acid, uric acid, creatine, and creatinine were only consumed, whereas urea, sarcosine, and glycine intermediates were both produced and

dx.doi.org/10.1021/jf401212n | J. Agric. Food Chem. 2013, 61, 6175−6186

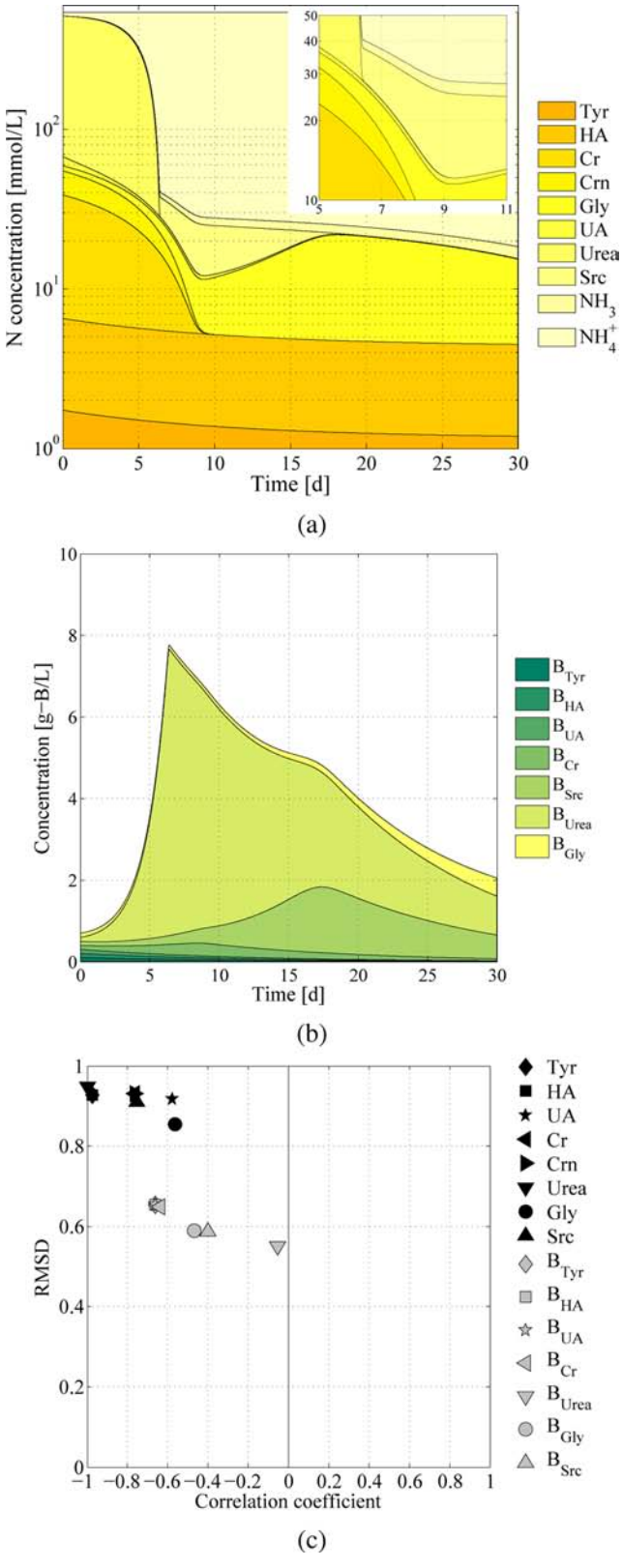

Figure 4. (a) OAC concentration, (b) microbial biomass concentration, and (c) affinity of OACs and microorganism concentration with the conversion factor f_{con} expressed by the root-mean-square distance RMSD and correlation coefficient R. Results refer to an instantaneous amendment of 1 L of urine at dilution D = 1 over 30 days.

consumed, during urine breakdown. However, urea was consumed more rapidly than it was produced, whereas sarcosine and glycine underwent an increase followed by a decrease in concentration. Among the OACs, urea was rapidly consumed in the first 5−6 days, whereas NH_3 and NH_4^+ were concurrently produced and became the most important species with only trace amounts of all other OACs after 5 days. The microbial biomass underwent an increase, especially high for B_{Gly}, B_{urea}, and B_{Src}, and a decrease after about 6−18 days, respectively. The correlation coefficient, R, and root-mean-square distance, RMSD, were calculated between each compound and each microbial group with respect to f_{con}, each being first normalized by their maximum value for comparison. The plot in Figure 4c shows that f_{con} was generally more (negatively) correlated with OACs than microorganism concentration, but also shows that the latter had lower values of RMSD to f_{con}. The compounds with the strongest correlation with f_{con} were urea, the major NH_3 and NH_4^+ supplier when consumed by bacteria, tyrosine (Tyr), and hippuric acid (HA).

Urine degradation dynamics after pulses also depend on the initial microbial biomass concentration. Soil microorganisms that mediate the reactions in eqs 1−8 are expected not to be limited to the strains used in the experiments described under Experimental Data and Parameter Estimation, but many more strains are likely to perform them. Because of this, we have explored how initial microbial concentration influenced the overall urine degradation cycle over 30 days with the total initial microbial biomass ranging between 0.1 and 100 g L^{-1} (a cumulative of about 32 g L^{-1} was found from parameter estimation).

The map in Figure 5 represents f_{con} as a function of time and total initial biomass (colored area) and demonstrates that high biomass concentrations led to very rapid urine degradation and conversion to NH_3 and NH_4^+, with up to a net 90% converted to assimilable N within the first 2−3 days for an initial biomass between 10 and 100 g L^{-1}. An initial biomass content smaller

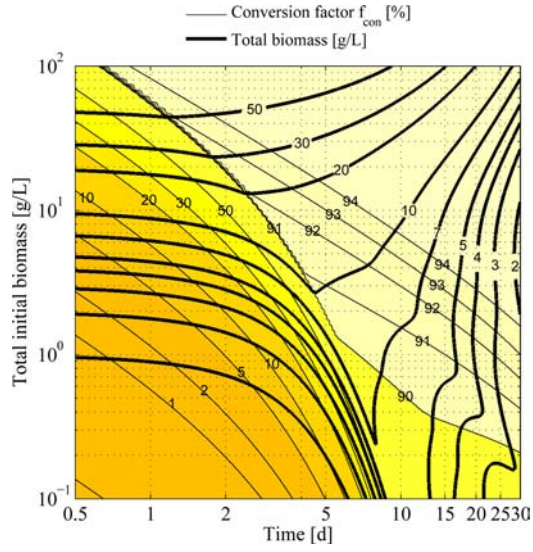

Figure 5. Modeled net N conversion factor f_{con} of total N to NH_3-N and NH_4^+-N for total initial biomass concentration ranging between 0.1 and 100 g L^{-1} (colored area) over 30 days following an instantaneous application of 1 L of human urine in soils with initial OACs concentration corresponding to natural average contents in human urine.

dx.doi.org/10.1021/jf401212n | J. Agric. Food Chem. 2013, 61, 6175−6186

than 1 g L^{-1} resulted in a slower net conversion, which reached 90% in a time ranging from about 5 to >30 days. Likewise, in Figure 3, the total biomass concentration in Figure 5 reached a maximum, beyond which it decreased. The maximum biomass occurred in correspondence to f_{con} between 80 and 90% for total initial biomass concentrations smaller than about 40 g L^{-1}, but a maximum was not detected above 40 g L^{-1}.

Continuous Amendments. Continuous-in-time urine amendments were analyzed to highlight features in degradation dynamics appearing over a large time scale, when the system reached steady state. Because of the steady state, the initial microbial biomass and OAC concentration were not relevant, whereas the key parameters controlling the system were the urine flow rate, F, and its dilution, D. For these analyses, a set of simulations were run over 120 days for D in the range from 0.1 to 10 and for the flow rate, F, from 0.01 to 10 L day^{-1}, which corresponded to a turnover time, T, ranging from 100 to 0.1 days, respectively.

Urine degradation to NH_3 and NH_4^+ was highly nonlinear with D and F (color area) and showed no strong correlation with the total biomass (thick black lines in in Figure 6). The highest conversion, f_{con}, occurred at low dilutions ($D < 1$) and low flow rates ($F < 1$ L day^{-1}), which corresponded to long turnover time ($T > 1$ day). In contrast, the highest microbial biomass appeared to occur at high urine concentrations ($D > 1$) and high flow rates ($F > 1$ L day^{-1}). This result can be explained by the long turnover time (i.e., low rate of incoming N), which led to near-full consumption of available substrates regardless of the biomass concentration. Conversely, short turnover times corresponded to high rate of nutrient recharge that, despite feeding microorganisms and allowing them to grow more than in the other cases, led to lower f_{con} values. To further support our explanation of these results, we observed that the microbial biomass was highly correlated with the total N inflow rate, as lines of equal biomass content were nearly aligned with lines of equal N inflow (dashed black lines). These lines also show that the equilibrium total biomass concentrations were reached at the corresponding lines of equal N input rate and show that the system was at the steady state.

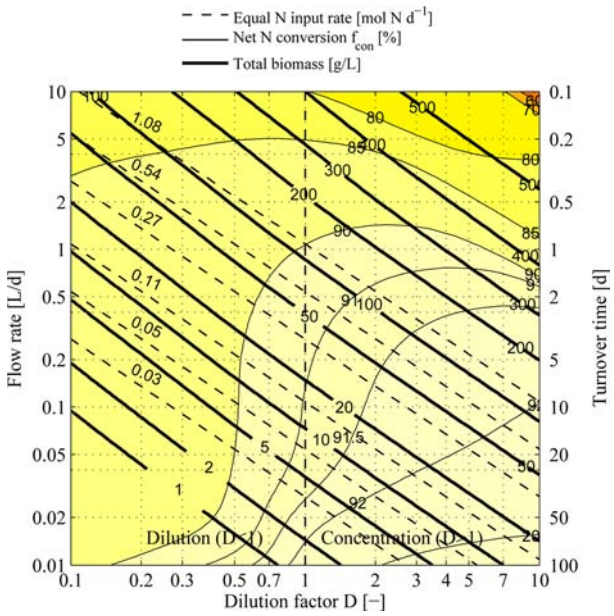

Figure 6. Modeled net conversion factor f_{con} of total N to NH_3-N and NH_4^+-N forms (colored area) and total microbial biomass (thick black lines) as a function of urine dilution D and flow rate F at steady state obtained at 120 days.

Stochastic Sensitivity Analyses. An analysis of the sensitivity of OAC biodegradation reactions was carried out within the framework of stochastic parameter uncertainty. For these analyses, the sensitivity to variability in Michaelis–Menten constants (K_X) and reaction rate constants (μ_X) was decoupled and analyzed assuming that uncertainty can be described by a Gaussian distribution function according to the central limit theorem. To this aim, values of μ_X and K_X were randomly extracted from a Gaussian distribution function with average equal to the values obtained by parameter estimation and standard deviation equal to ±1, ±5, and ±10% their average. For these analyses, 1000 realizations were generated for each level of uncertainty and for each parametric group.

Panels a and b of Figure 7 show that uncertainty in the Michaelis–Menten constants K_X affected only marginally the net N conversion factor f_{con} and the total biomass for urine applications consisting of a single pulse of 1 L of urine at natural average OAC concentrations. Similarly, uncertainty in the reaction rate constant μ_X in Figure 7c,d had a relatively small effect at ±1 and ±5% and only marginally affected OAC conversion f_{con} and total biomass at ±10%. Overall, we note that variability in μ_X was small, even if it was a bit larger than the variability in K_X.

A similar analysis was carried out for a continuous flow of 1 L day^{-1} of urine at natural average OAC concentration. Figure 8 shows results similar to those in Figure 7, but also highlights that uncertainties in μ_X and K_X for continuous flows led to higher model uncertainty than for a single pulse. In fact, the total biomass showed large standard deviations for variability in both K_X and μ_X.

DISCUSSION

The reaction network and dynamics of human urine decomposition in soil proposed here were tested to determine the release amount, timing, and rate of N end-products from breakdown of organic amino compounds. Necessarily, some assumptions had to be taken and are discussed here in more detail.

Whereas the reaction network proposed in Figure 1 included OACs, OASs, and ISs, the mathematical model explicitly included only OACs. The purpose of this work was to demonstrate key dynamical features arising from biochemical breakdown that depended on kinetic processes, whereas OASs and ISs were mostly determined by equilibrium parameters and did not imply biochemical reactions directly.

The microbial functional groups included in the model were assumed to exert only one reaction, each relative to one OAC substrate, but we have no evidence as yet on whether multiple reactions within the proposed network can be expressed by the same functional group. It is likely that a low concentration of a preferred substrate induces microorganisms to switch to a different substrate that has similar C and N contents; however, in such a case, there is no knowledge of whether biochemical parameters would change. These metabolic characteristics were not included in the model and require further case-specific investigation. On a biochemical level, the catabolic (substrate breakdown) and anabolic (biomass accretion) pathways of each reaction were simplified and represented by one pathway under the assumption that energy and mass were conserved. These features harmonized with the mathematical simplification of the

dx.doi.org/10.1021/jf401212n | J. Agric. Food Chem. 2013, 61, 6175–6186

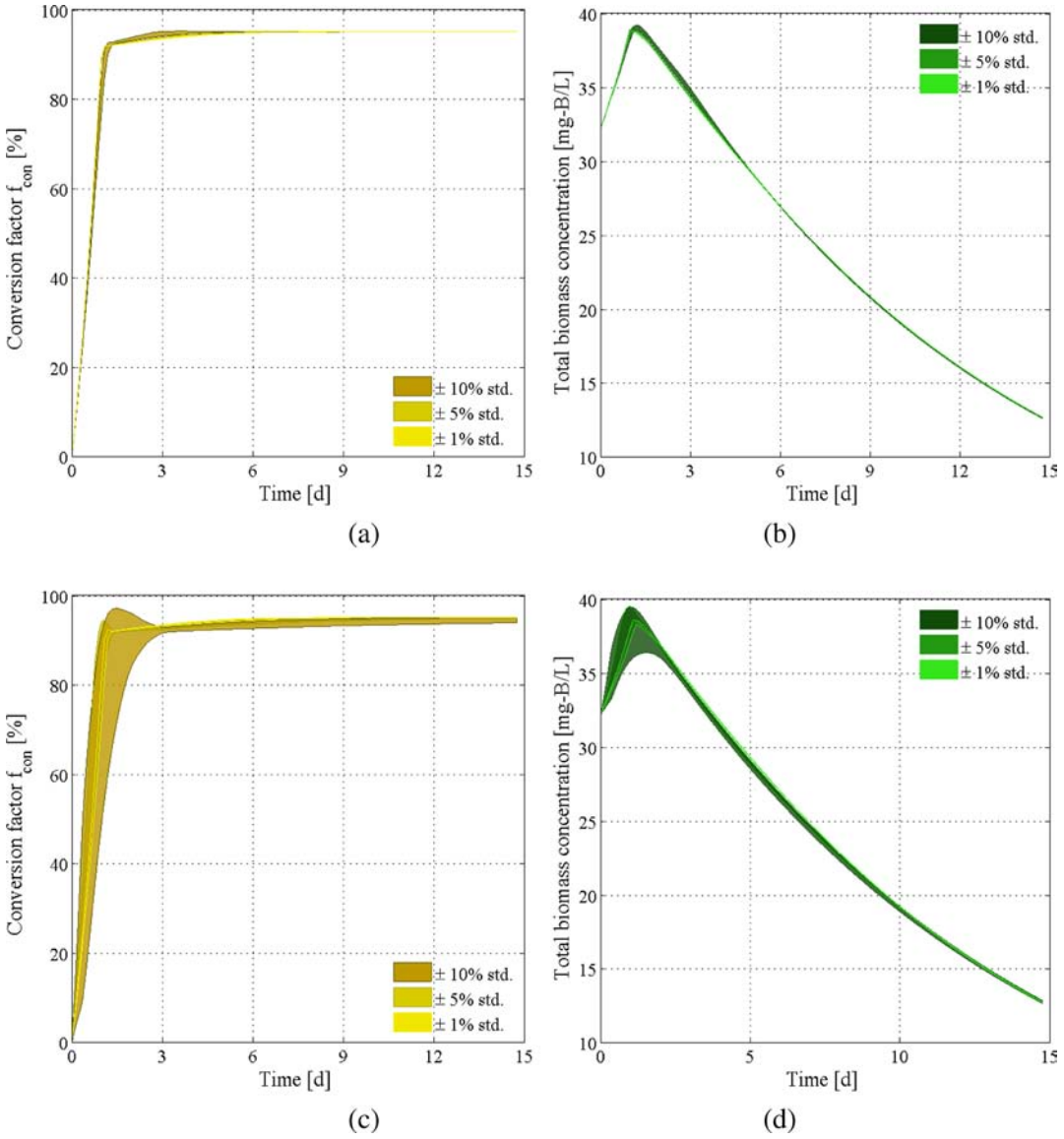

Figure 7. Stochastic sensitivity analysis of net N conversion factor f_{con} and total microbial biomass to variability in Michaelis–Menten constants (a and b, respectively) and reaction rate constants (c and d, respectively). Parameter variability ranged between ±1, ± 5, and ±10%. Simulations corresponded to the system response to a pulse application of 1 L of urine at natural average OACs concentration.

system; in fact, not the individual bacterial strains but, rather, bacterial functional groups were modeled; that is, strains that showed, or were assumed to show, metabolic similarities against the OACs considered here were grouped (e.g., typical strains used in experimental cultures belong to *Pseudomonas*). We have no proof that this could be the only way to represent to microbial communities and their metabolic functioning, but we can infer that reaction pathways could change for different interactions among microbial strains and functional groups as per microbial ecology.

The model excluded metals excreted with urine as these have low concentrations.[14] However, when the model is to be interrogated on the capability to match nutrient demand by plants, uptake of free ions (included in the reaction network) and metals (not included) must be implemented in the model after tests to gather experimental data of primary, secondary, and micro nutrient plant and microbe uptake.[36]

The average human urine content of OACs, OASs, and ISs is very largely dependent on the feeding behavior, including water and protein intake. Worldwide, the feeding behavior can be substantially different from region to region, with developed countries taking in more proteins from meats than developing countries.[2] Therefore, large variabilities in the total and relative OACs concentrations are expected to depend on the geographical area. As such, the effectiveness of urine fertilization and the release rate of NH_3 and NH_4^+ may vary. In addition to the variability in OACs, OASs, and ISs, human urine may convey substances derived by medicaments that are not or partially metabolized and that can be taken up by plants[57] and high concentrations of estrogen hormones that can affect the microfauna.[58] An understanding of the effects of drug-derived substances on soil biochemistry, microbial biomass, and plants is currently unavailable, and this will be one of the most important aspects that has to be investigated if large-scale infrastructures for urine diversion are to be designed and constructed for uses in agriculture[11,59] and aquaculture.[14,60]

A concern with urine fertilization is represented by the high concentrations of NaCl and other salts (see Table 1). As salts

dx.doi.org/10.1021/jf401212n | J. Agric. Food Chem. 2013, 61, 6175–6186

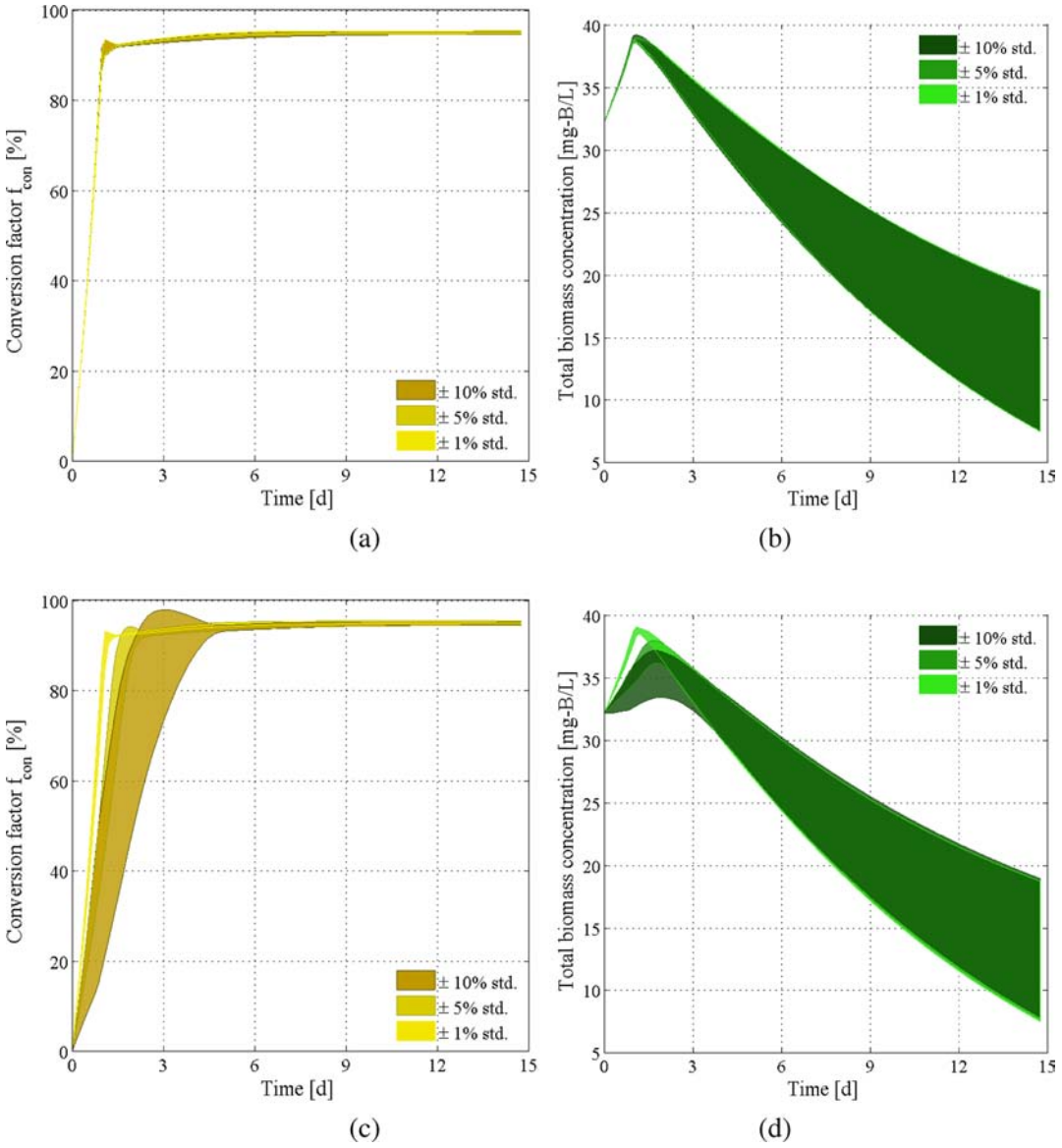

Figure 8. Stochastic sensitivity analysis of net N conversion factor f_{con} and total microbial biomass to variability in Michaelis–Menten constants (a and b) and reaction rate constants (c and d). Parameter variability ranged between ±1, ±5, and ±10%. Simulations corresponded to the system response to a continuous flow rate of 1 L day^{-1} of urine at natural average OACs concentration.

may accumulate in the soil over long time scales, a regular rotation of salt-tolerant or salt-accumulating crops may be required to contain soil salinity buildup. For example, Mnkeni et al.[6] did not observe yield reduction with maize, tomato, and beetroot, but found that the yield for carrots was decreased with high urine fertilization rates. Jonsson et al.[4] suggested the use of diluted urine for fertilization to reduce salt concentrations or to irrigate after fertilization to limit possible detrimental effect of salts on crops. For naturally saline soils, fertilization procedures need to be evaluated to contain further increases in soil salinity. Given the large variety of salt-tolerant crops,[37] the use of our model, when coupled with specific crops, could account for the uptake of ions such as Na^+, K^+, and Cl^- as well as investigate the effect of urine application over multiple years.

Overall, according to our model, 90% of the incoming N was converted to NH_3 and NH_4^+ in a time ranging from 5 to 20 day for instantaneous applications, but conversion could occur more rapidly or slowly depending on the microbial biomass concentration. For continuous applications, 90% or more conversion to NH_3 and NH_4^+ occurred at 120 days for flow rates smaller than 2 L day^{-1} regardless of the dilutions. As expected, urea had the highest correlation with the release of NH_3 and NH_4^+ among all compounds because urea has the highest concentration, but our results showed that also other compounds, more complex than urea, contribute to the urine biogeochemical cycle. Finally, stochastic analyses confirmed that microbial growth rates were a larger source of uncertainty as compared to Michaelis–Menten concentrations.

This work presents the basis for further investigations at both the mathematical and experimental level on the opportunity to reuse human urine as a source of agricultural nutrient and move toward more sustainable resource management.

APPENDIX

The set of ordinary differential equations describing the reactions in Figure 1 is

dx.doi.org/10.1021/jf401212n | J. Agric. Food Chem. 2013, 61, 6175–6186

$$\frac{d[Tyr]}{dt} = -M_{Tyr} + S_{Tyr} \quad (16a)$$

$$\frac{d[HA]}{dt} = -M_{HA} + S_{HA} \quad (16b)$$

$$\frac{d[UA]}{dt} = -M_{UA} + S_{UA} \quad (16c)$$

$$\frac{d[Cr]}{dt} = -M_{Cr} + \frac{1}{k_{d,Cr}}\frac{d[Crn]}{dt} + S_{Cr} \quad (16d)$$

$$\frac{d[Crn]}{dt} = k_{d,Cr}\frac{d[Cr]}{dt} + S_{Crn} \quad (16e)$$

$$\frac{d[Src]}{dt} = -M_{Src} + M_{Cr} \quad (16f)$$

$$\frac{d[Gly]}{dt} = -M_{Gly} + M_{Src} + S_{Gly} \quad (16g)$$

$$\frac{d[urea]}{dt} = \frac{1}{2}M_{Tyr} + \frac{1}{2}M_{HA} + M_{Cr} + 2M_{UA} - M_{urea} + S_{urea} \quad (16h)$$

$$\frac{d[NH_3]}{dt} = M_{Gly} + k_{d,NH_4^+}\frac{d[NH_4^+]}{dt} + S_{NH_3} \quad (16i)$$

$$\frac{d[NH_4^+]}{dt} = 2M_{urea} + \frac{1}{k_{d,NH_4^+}}\frac{d[NH_3^+]}{dt} \quad (16j)$$

$$\frac{dB_X}{dt} = Y_X M_X I - \delta_X B_X \quad (16k)$$

where the Michaelis–Menten term M_X for compound X is

$$M_X = \mu_X \frac{[X]}{K_X + [X]}\frac{B_X}{Y_X}$$

and the biomass inhibition I is as in eq 11

AUTHOR INFORMATION

Corresponding Author

*(F.M.) E-mail: federico.maggi@sydney.edu.au. Phone: +61 (0)2 93512115. Fax: +123 (0)2 9251.

Notes

The authors declare no competing financial interest.

ACKNOWLEDGMENTS

We thank Nathan Guerry for his contribution to the initial development of this project, who was supported by the Summer Scholarship Programme of the School of Civil Engineering, The University of Sydney.

ABBREVIATIONS USED

OAC, organic amino compound; OAS, organic ammonium salt; IS, inorganic salt; *R*, correlation coefficient; RMSD, root-mean-square distance

REFERENCES

(1) Udert, K. M.; Larsen, T. A.; Gujer, W. *Water Sci. Technol.* **2006**, *54*, 413–420.

(2) Mihelcic, J. R.; Fry, L. M.; Shaw, R. *Chemosphere* **2011**, *84*, 832–839.

(3) Larsen, T. A.; Alder, A. C.; Eggen, R. I. L.; Maurer, M.; Lienert, J. *Environ. Sci. Technol.* **2009**, *43*, 6121–6125.

(4) Jonsson, H.; Stintzing, A.; Vinneras, B.; Salomon, E. *Guidelines on the Use of Urine and Faeces in Crop Production*; EcoSanRes Publication Series, Stockholm Environment Institute: Stockholm, Sweden, 2004; Vol. 2004-2.

(5) Jensen, P. K. M.; Phuc, P. D.; Knudsen, L. G.; Dalsgaard, A.; Konradsen, F. *Int. J. Hyg. Environ. Health* **2008**, *211*, 432–439.

(6) Mnkeni, P. N. S.; Kutu, F. R.; Muchaonyerwa, P.; Austin, L. M. *Waste Manage. Res.* **2008**, *26*, 132–139.

(7) Heinonen-Tanski, H.; van Wijk-Sijbesma, C. *Bioresour. Technol.* **2005**, *96*, 403–411.

(8) Karak, T.; Bhattacharyya, P. *Resourc., Conserv. Recycl.* **2011**, *55*, 400–408.

(9) Vinneras, B. *Faecal Separation and Urine Diversion for Nutrient Management of Household Biodegradable Waste and Wastewater*; Swedish University of Agricultural Sciences: Uppsala, Sweden, 2001; Vol. 244.

(10) Lienert, J.; Haller, M.; Berner, A.; Stauffacher, M.; Larsen, T. A. *Water Sci. Technol.* **2003**, *48*, 47–56.

(11) Kirchmann, H.; Pettersson, S. *Fertilizer Res.* **1995**, *40*, 149–154.

(12) Pradhan, S. K.; Nerg, A. M.; Sjoblom, A.; Holopainen, J. K.; Heinonen-Tanski, H. *J. Agric. Food Chem.* **2007**, *55*, 8657–8663.

(13) Guzha, E.; Nhapi, I.; Rockstrom, J. *Phys. Chem. Earth* **2005**, *30*, 840–845.

(14) Adamsson, M. *Ecol. Eng.* **2000**, *16*, 243–254.

(15) Pradhan, S. K.; Holopainen, J. K.; Heinonen-Tanski, H. *J. Agric. Food Chem.* **2009**, *57*, 7612–7617.

(16) Pradhan, S. K.; Holopainen, J. K.; Weisell, J.; Heinonen-Tanski, H. *J. Agric. Food Chem.* **2010**, *58*, 2034–2039.

(17) Pradhan, S. K.; Pitkanen, S.; Heinonen-Tanski, H. *Agric. Food Sci.* **2010**, *19*, 57–67.

(18) Antonini, S.; Nguyen, P. T.; Arnold, U.; Eichert, T.; Clemens, J. *Sci. Total Environ.* **2012**, *414*, 592–599.

(19) Akpan-Idiok, A. U.; Udo, I. A.; Braide, E. I. *Resourc., Conserv. Recycl.* **2012**, *62*, 14–20.

(20) Putnam, D. *Composition and Concentrative Properties of Human Urine*; NASA: Huntington Beach, CA, 1971; Vol. NASA CR-1802.

(21) Gregor, O.; Schuck, O. *Am. J. Dig. Dis.* **1957**, *2*, 110–115.

(22) Bachrach, U. *J. Gen. Microbiol.* **1957**, *17*, 1–11.

(23) Schefferle, H. *J. Appl. Bacteriol.* **1965**, *28*, 412.

(24) Karlsson, J. L.; Barker, H. A. *J. Biol. Chem.* **1949**, *178*, 891–902.

(25) Bloch, K.; Schoenheimer, R. *J. Biol. Chem.* **1939**, *131*, 111–119.

(26) Wyss, M.; Kaddurah-Daouk, R. *Physiol. Rev.* **2000**, *80*, 1107–1213.

(27) Kaplan, A.; Naugler, D. *Mol. Cell. Biochem.* **1974**, *3*, 9–15.

(28) Yamada, H.; Shimizu, S.; Kim, J. M.; Shinmen, Y.; Sakai, T. *FEMS Microbiol. Lett.* **1985**, *30*, 337–340.

(29) Shimizu, S.; Kim, J. M.; Shinmen, Y.; Yamada, H. *Arch. Microbiol.* **1986**, *145*, 322–328.

(30) Appleyard, G.; Woods, D. D. *J. Gen. Microbiol.* **1956**, *14*, 351–365.

(31) Nimmosmith, R. H.; Appleyard, G. *J. Gen. Microbiol.* **1956**, *14*, 336–350.

(32) Reoch, J. *J. Anatomy Physiol.* **1875**, *9*, 368–385.

(33) Warner, R. C. *J. Biol. Chem.* **1942**, *142*, 705–723.

(34) Chin, W.-t.; Kroontje, W. *Soil Sci. Soc. Am. J.* **1963**, *27*, 316–318.

(35) Mobley, H. L. T.; Hausinger, R. P. *Microbiol. Rev.* **1989**, *53*, 85–108.

(36) Heard, J.; Hay, D. In *Nutrient content, uptake and carbon: nitrogen ratios of prairie crops*, Manitoba Agronomists Conference 2006, University of Manitoba: Winnipeg, Manitoba , December 12–13, 2006 (http://umanitoba.ca/faculties/afs/MAC_proceedings/proceedings/2006/heard_hay_nutrient_uptake.pdf).

(37) Brady, N. C.; Weil, R. R. *The Nature and Properties of Soils*, 12th ed.; Prentice-Hall: Upper Saddle River, NJ, 1999.

(38) Rosswall, T. *Plant Soil* **1982**, *67*, 15–34.

(39) Maggi, F.; Gu, C.; Riley, W. J.; Hornberger, G. M.; Venterea, R. T.; Xu, T.; Spycher, N.; Steefel, C.; Miller, N. L.; Oldenburg, C. M. *J. Geophys. Res.—Biogeosci.* **2008**, *113*, G02016 (doi: 10.1029/2007JG000578).
(40) Brimblecombe, P. In *Treatise on Geochemistry*; Schlesinger, W., Ed.; Elsevier: Amsterdam, 2003; Vol. 8, 645–682, p 720.
(41) Atkins, P. W. *Physical Chemistry*, 6th ed.; Oxford University Press: Oxford, UK, 1998.
(42) Monod, J. *Annu. Rev. Microbiol.* **1949**, *3*, 371–394.
(43) Bekins, B. A.; Warren, E.; Godsy, E. M. *Ground Water* **1998**, *36*, 261–268.
(44) Stewart, T. L.; Fogler, H. S. *Biotechnol. Bioeng.* **2002**, *77*, 577–588.
(45) Stewart, T. L.; Kim, D. S. *Biochem. Eng. J.* **2004**, *17*, 107–119.
(46) Maggi, F.; Porporato, A. *Water Resourc. Res.* **2007**, *43*, W07444 (doi: 10.1029/2006WR005367, 2007.
(47) Ross, K. F. A.; Billing, E. *J. Gen. Microbiol.* **1957**, *16*, 418.
(48) Wolery, T. EQ3/6, A Software Package for Geochemical Modeling of Aqueous Systems: Package Overview and Installation Guide (Version 7.0), Lawrence Livermore National Laboratory, University of California, Livermore, CA, 1992.
(49) Sui, Y.-Y.; Yan, L.; Xu, A.; Zhang, L.; Wang, S.; Guan, L.-Z. *Chinese J. Soil Sci.* **2010**, *41*, 4.
(50) Bhat, M.; Murthy, D.; Saidutta, M. *J. Agric. Biol. Sci.* **2011**, *6*, 60–63.
(51) Chiellini, E.; Corti, A.; D'Antone, S.; Billingham, N. C. *J. Polym. Environ.* **2007**, *15*, 169–178.
(52) Gastrin, B.; Kallings, L. O.; Marcetic, A. *Acta Pathol. Microbiol. Scand.* **1968**, *74*, 371–380.
(53) Salem, S.; Moussa, M. S.; van Loosdrecht, M. C. M. *Biotechnol. Bioeng.* **2006**, *94*, 252–262.
(54) Kim, S. B. *Hydrol. Processes* **2006**, *20*, 1177–1186.
(55) Clapp, R. B.; Hornberger, G. M. *Water Resour. Res.* **1978**, *14*, 601–604.
(56) Brooks, R. H.; Corey, A. T. *Hydrology Paper 3*; Colorado State University: Fort Collins, CO, 1964
(57) Winker, M.; Clemens, J.; Reich, M.; Gulyas, H.; Otterpohl, R. *Sci. Total Environ.* **2010**, *408*, 1902–1908.
(58) Lucas, S. D.; Jones, D. L. *Soil Biol. Biochem.* **2009**, *41*, 236–242.
(59) Cabrera, M. L.; Kissel, D. E.; Bock, B. R. *Soil Biol. Biochem.* **1991**, *23*, 1121–1124.
(60) Jana, B. B.; Rana, S.; Bag, S. K. *Water Sci. Technol.* **2012**, *65*, 1350–1356.